Biochimica et Biophysica Acta, 1015 (1990) 96–108
Elsevier

BBABIO 43104

Charge recombination between the oxidized high-potential *c*-type cytochromes and Q_A^- in reaction centers from *Rhodopseudomonas viridis*

Ji-Liang Gao, Robert J. Shopes * and Colin A. Wraight

Department of Physiology and Biophysics and Department of Plant Biology, University of Illinois, Urbana, IL (U.S.A.)

(Received 7 August 1989)

Key words: Photosynthesis; Reaction center; Cytochrome; Charge recombination; Electron transfer; (*Rps. viridis*)

Isolated reaction centers from *Rhodopseudomonas viridis* contain two high-potential *c*-type cytochromes, cytochrome *c*-559 and cytochrome *c*-556, and two low potential *c*-type cytochromes, cytochrome *c*-552 and cytochrome *c*-554. At moderate redox potentials, the two low-potential cytochromes are oxidized and are not identifiably involved in light-induced turnover. Following a flash, in the absence of functional secondary acceptor quinone, Q_B, the charge separation states, $C_{H2}^+C_{H1}Q_A^-$ and $C_{H2}^+C_{H1}^+Q_A^-$ are rapidly created, where C_{H1} is cytochrome *c*-559 and C_{H2} is cytochrome *c*-556. Decay of these two states occurs via slow intramolecular charge recombinations. The rates of recombination for the two states were distinguishable and were pH and temperature dependent. At pH 9 and 296 K, $k_{H1}^{app} = 8.5 \pm 0.5\ s^{-1}$ for the charge recombination of $C_{H2}^+C_{H1}^+Q_A^-$ and $k_{H2}^{app} = 0.95 \pm 0.05\ s^{-1}$ for the charge recombination of $C_{H2}^+C_{H1}Q_A^-$. It was suggested that the mechanism for decay of both cytochrome $c^+Q_A^-$ states is via repopulation of the $P^+Q_A^-$ state, where P is the primary donor, followed by rapid (ms) recombination of this state, with a rate k_P. Recovery of $C_{H2}^+C_{H1}Q_A^-$ also requires thermal equilibrium between the two hemes: $C_{H2}^+C_{H1} \leftrightarrow C_{H2}C_{H1}^+$. In addition to these indirect paths, there is a direct route of recovery for each of the states, $C_{H2}^+C_{H1}Q_A^-$ and $C_{H2}^+C_{H1}^+Q_A^-$. The direct pathways are evident at low temperature when the recovery processes become almost temperature independent, below about 220 K. In 60% ethylene glycol, the limiting rates are: $k_{H1}^0 = 1.85\ s^{-1}$ for $C_{H2}^+C_{H1}^+Q_A^-$, and $k_{H2}^0 = 0.15\ s^{-1}$ for $C_{H2}^+C_{H1}Q_A^-$. That these rates differ by only a factor of 10 is remarkable in view of the 30 Å (center-to-center) separation between the two high-potential hemes and the involvement of intermediate states is briefly considered. From the model, the calculated rates, at any temperature, are given by: $k_{H1}^{app} = (k_P + K_c k_{H1}^0)/(1 + K_c)$ for $C_{H2}^+C_{H1}^+Q_A^-$ recombination, and $k_{H2}^{app} = [k_P + K_c(k_{H1}^0 + K_e k_{H2}^0)]/[1 + K_c(1 + K_e)]$ for $C_{H2}^+C_{H1}Q_A^-$ recombination, where K_c is the equilibrium constant for the positive hole to lie on either P or C_{H1}, and K_e is the equilibrium constant for electron transfer between the two high-potential cytochromes, C_{H1} and C_{H2}. Equilibrium redox titrations distinguished the two high-potential cytochromes *c* and revealed their distinct pH and temperature dependences. K_c was taken from the difference in the measured equilibrium midpoint potentials (ΔE_m) of the C_{H1}^+/C_{H1} and P^+/P couples, and K_e was taken from ΔE_m for C_{H2}^+/C_{H2} and C_{H1}^+/C_{H1}. The rate of $P^+Q_A^-$ decay, k_P, was taken from measurements when all *c*-type cytochromes were chemically oxidized, and this was used to approximate the rate when the high-potential cytochromes were reduced. All three variable parameters were measured over a range of pH and temperature, and the calculated rates were compared to experimental rates determined under these conditions. The agreement between calculated and measured values was good and provides strong support for the proposed mechanism. The adequacy of equilibrium E_m values and the measured value of k_P is discussed in terms of possible electrostatic interactions between charged redox centers. It is concluded that such interactions are of minor importance for all relevant parameters in isolated reaction centers.

* Present address: Department of Cell Biology, Stanford University, Palo Alto, CA 94305, U.S.A.

Abbreviations: RC, reaction center; Mops, 4-morpholinepropanesulfonic acid; CAPS, 3-[cyclohexylamino]-1-propanesulfonic acid; CHES, 2-[*N*-cyclohexylamino]ethanesulfonic acid.

Correspondence: C.A. Wraight, Department of Plant Biology, University of Illinois, 289 Morrill Hall, 505 S. Goodwin Avenue, Urbana, IL 61801, U.S.A.

Introduction

In addition to subunits L, M and H, common to reaction centers from many photosynthetic bacteria, the reaction center from *Rhodopseudomonas viridis* contains a tightly bound, four-heme cytochrome *c* subunit [1–5]. Absorption of a photon by the reaction center results in photooxidation of the primary donor, P, and reduction of the primary acceptor quinone, Q_A. The four cytochromes *c* function as secondary donors to P^+ [1,2]. It is well known that two of them are low-potential and two are high-potential [3]. The 3-dimensional structure of the *Rps. viridis* reaction center, obtained from X-ray diffraction studies, shows that the four hemes are lined up in series behind P and, therefore, are inequivalent in position [4,5]. The four hemes have recently been characterized with respect to spectra and kinetics. After a short flash, one of the high-potential cytochromes, cytochrome *c*-559, which is believed to lie closest to P, donates an electron to P^+ with a rate of $3.7 \cdot 10^6$ s^{-1}; the other high-potential cytochrome, cytochrome *c*-556, donates an electron to cytochrome c^+-559 with a rate of $2.8 \cdot 10^5$ s^{-1} [6,7]. In much of what follows, cytochrome *c*-559 and cytochrome *c*-556 will be referred to as C_{H1} and C_{H2}, respectively, and collectively as cytochrome *c*.

At moderate redox potential, the two low-potential cytochromes *c* are oxidized and, therefore, after a flash only the two high-potential cytochromes *c* (C_{H1} and C_{H2}) can donate an electron to P^+. In isolated reaction centers containing only Q_A, the charge separation states, $C^+_{H2}C^+_{H1}Q^-_A$ or $C^+_{H2}C_{H1}Q^-_A$ (depending on E_h) are rapidly created following flash excitation. Previously, we showed that these states slowly recover via an intramolecular charge recombination [8] and similar kinetics have been observed in chromatophores and whole cells (Ref. 9; Fleischman, D., personal communication). However, their decay kinetics and thermal characteristics have not been fully described. In this paper we report on the pH and temperature dependences of the recovery kinetics of the two high-potential cytochromes and suggest a mechanism for the charge recombination reactions. The rates predicted from the model fit the measured data over a wide range of pH and temperature.

Materials and Methods

Reaction centers were prepared as previously described [8,10]. The secondary quinone acceptor, Q_B, was largely removed by the reaction center purification procedure. Residual Q_B activity was inhibited by *o*-phenanthroline (4 mM).

The experimental apparatus, a kinetic spectrophotometer for optical measurement in the ambient and low-temperature ranges, was as previously described [11,12]. The recovery kinetics of cytochrome c^+ were monitored at 558 nm and those of Q^-_A were measured by a double flash method [8]. The decay kinetics of cytochrome c^+ were fit to a biexponential and a constant, using a modified Marquardt analysis.

The redox potential was measured with a platinum electrode vs. an Ag|AgCl reference electrode. The redox potential was changed by small additions of ferricyanide and ascorbate. Three methods were used in redox titrations of the high potential cytochromes *c*. (1) Dark titrations: reduced high-potential cytochrome *c* was measured at 558 nm vs. an oxidized reference sample, in an Aminco DW-2 spectrophotometer. (2) Flash titrations: the amount of reduced high-potential cytochrome *c* at a given E_h was measured from the total absorbance change at 558 nm after four saturating flashes, in the kinetic spectrophotometer. (3) Kinetic titrations: the recovery kinetics were measured at different E_h, and the fast phase and slow phase components of the cytochrome *c* decay were obtained from a biexponential fit of the kinetic trace. Redox titrations of P were done by assaying the flash-induced P^+ signal at 450 nm. Redox titration curves were analysed by computer for a best fit to one (P^+/P) or two (cytochrome c^+/cytochrome *c*) components.

The temperature dependence of the reference electrode (calomel, 4 M KCl; −0.36 mV per degree centigrade) was obtained by extrapolation of values in the literature for 0.1 M and 1.0 M KCl [13].

Results

Rereduction kinetics of cytochrome c^+

Fig. 1 shows the rereduction kinetics of cytochrome c^+ at three different redox potentials, following a saturating flash, at pH 9.0, 296 K. The two low-potential cytochromes *c* were oxidized at all redox potentials and secondary electron transfer to Q_B was blocked by

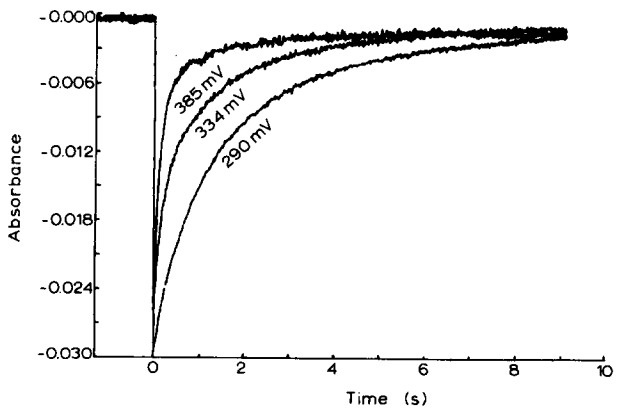

Fig. 1. The recovery kinetics of photooxidized high potential cytochrome c^+, measured at 558 nm. 2 μM reaction center, 100 mM NaCl, 0.05% Triton X-100, 4 mM *o*-phenanthroline, 10 mM CHES (pH 9.0); $T = 296$ K. The three curves were measured at different redox potentials (385, 334 and 290 mV) as indicated in the figure.

o-phenanthroline. In general, the decay curves could be well fit by the sum of two exponentials and a small constant, leaving no visible residuals. The magnitude of the constant component in the best fit was very small at room temperature (less than 5% of the total) and its origin was not investigated. At 296 K (pH 9.0), over a range of redox potentials, the two components exhibited rate constants of 0.95 ± 0.05 s^{-1} and 8.5 ± 0.5 s^{-1}. However, the relative amplitudes of the two components varied with the redox potential of the sample so that the apparent (net) rate of recovery accelerated as the redox potential was raised. In Fig. 1, the relative amplitudes of the slow component were 80%, 50% and 20% when the redox potentials were 290 mV, 334 mV and 385 mV, respectively (see Fig. 1). In the following, the rate constants of the two decay kinetics will be denoted k_{slow} and k_{fast}, and their relative amplitudes, A_{slow} and A_{fast}.

pH dependence of the recovery kinetics of cytochrome c^+ and Q_A^-

The recovery rates of the oxidized high-potential cytochromes *c* following a saturating flash were measured as a function of pH at 296 K (Fig. 2). The redox potential of the sample was adjusted to be near the midpoint potential of cytochrome *c*-556 (between 250 mV and 350 mV) so that both kinetic components of the high-potential cytochrome recovery, fast and slow, could be measured simultaneously. The rate of the fast component, k_{fast}, was about 3.2 s^{-1} at pH 6.0, and increased with increasing pH to a value of 18 s^{-1} at about pH 10. Above pH 10, the rate was almost constant. The rate of the slow component, k_{slow}, was about 0.29 s^{-1} at pH 6.0, and increased with increasing pH up to a maximum rate of 1.5 s^{-1} at pH 9.5. Above pH 9.5 the recovery of the slow component slowed to a rate of 0.33 s^{-1} at pH 11.0. The recovery kinetics of Q_A^- reoxidation, as measured by a double flash method [8], revealed two similar kinetic components, with similar pH dependences (Fig. 2), consistent with the intramolecular nature of the recovery process. Qualitatively similar behavior is seen for cytochrome c^+ recovery in chromatophores (Fleischman, D., unpublished observations).

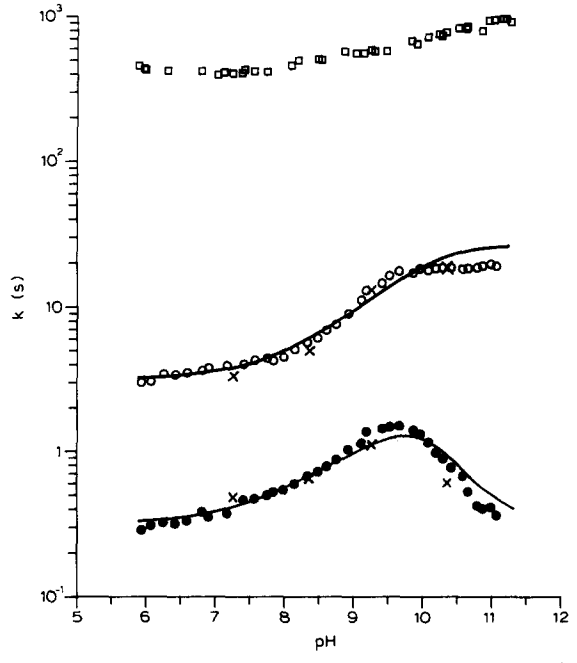

Fig. 2. The pH dependence of the rates of recovery of photoinduced cytochrome c^+. 2 μM reaction centers, 0.1% Triton X-100, 100 mM NaCl, 1 mM Tris, 20 μM ascorbate, 4 mM *o*-phenanthroline; $T = 296$ K. (○) Fast component: the rate of recovery of C^+_{H1}. (●) Slow component: the rate of the recovery of C^+_{H2}. The recovery kinetics of Q_A^- (×) were determined at pH 7.3, 8.4, 9.3 and 10.35 by a double flash method (Ref. 8) and are also plotted as fast and slow components. The rate of recovery of $P^+Q_A^-$, taken from Ref. 12, is also shown (□). The solid lines were constructed as described in the text, using Eqns. 1 and 2.

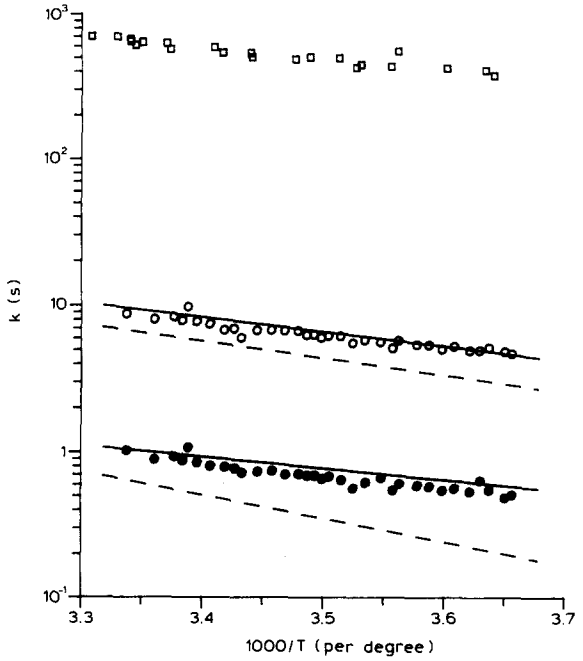

Fig. 3. The temperature dependence of the rate of recovery of photoinduced cytochrome c^+. 2 μM reaction centers, 0.05% Triton X-100, 100 mM NaCl, 10 mM CHES, 20 μM ascorbate, 4 mM *o*-phenanthroline (pH 9.0). (○) Fast component: the rate of recovery of C^+_{H1}. (●) Slow component: the rate of recovery of C^+_{H2}. The rate of recovery of $P^+Q_A^-$, taken from Ref. 12, is also shown (□). The solid lines were constructed as described in the text using Eqns. 1 and 2. The dashed lines indicate the slopes after subtraction of the limiting low-temperature process, as described in the text.

Temperature dependence of the recovery kinetics of cytochrome c^+

The temperature dependence of the high potential cytochrome c^+ decay kinetics was measured in aqueous buffer at pH 9.0 between 300 and 270 K (Fig. 3). The rate of the fast component was 9.0 s^{-1} at 300 K and

decreased with decreasing temperature to a rate of 4.5 s^{-1} at 273 K. The rate of the slow component was 1.0 s^{-1} at 300 K and also decreased with decreasing temperature, to a rate of 0.5 s^{-1} at 273 K. In this temperature range, the rates in 60% ethylene glycol were about 10–15% slower and the temperature dependences were very similar (data not shown).

Extended temperature dependences were done in 60% ethylene glycol, to allow freezing of the sample down to low temperature (Fig. 4A and B). The recovery rate of the fast component was 8 s^{-1} at 295 K, and declined to 1.8 s^{-1} at about 210 K. The rate then increased slightly, to 2.3 s^{-1} at 190 K, and remained at this value as the temperature was lowered further (Fig. 4A, open circles). For the slow component, the recovery rate was 0.8 s^{-1} at 295 K, decreasing to 0.15 s^{-1} and becoming almost temperature independent below 220 K (Fig. 4A, filled cycles).

Fig. 4B shows how the amplitudes of the two components varied with temperature. Above 250 K, the amplitudes of the fast and slow components exhibited antiparallel behavior – the amplitude of the fast component increased with decreasing temperature (open circles), while the amplitude of the slow component decreased with decreasing temperature (closed circles). Below 250 K both components decreased in parallel as the total amplitude of the recovery kinetics decreased. However, the relative contributions from the two components remained steady, at about 60% fast and 40% slow. In this temperature region, the two recovery components accounted for about 2/3 of the initial cytochrome oxidation. The remaining 1/3 recovered much more slowly and was not analyzed further. However, the temperature dependence of the amplitude of the initial oxidation, and of the amplitudes of the two recovery phases described, was reversible, implying that the slowly recovering portion did indeed recover in the time between measurements (about 5 min).

Equilibrium redox potential properties of cytochrome c-559 and cytochrome c-556

The equilibrium redox-potential properties of the high-potential cytochromes *c* were investigated by three methods. Dark titrations were performed in an Aminco

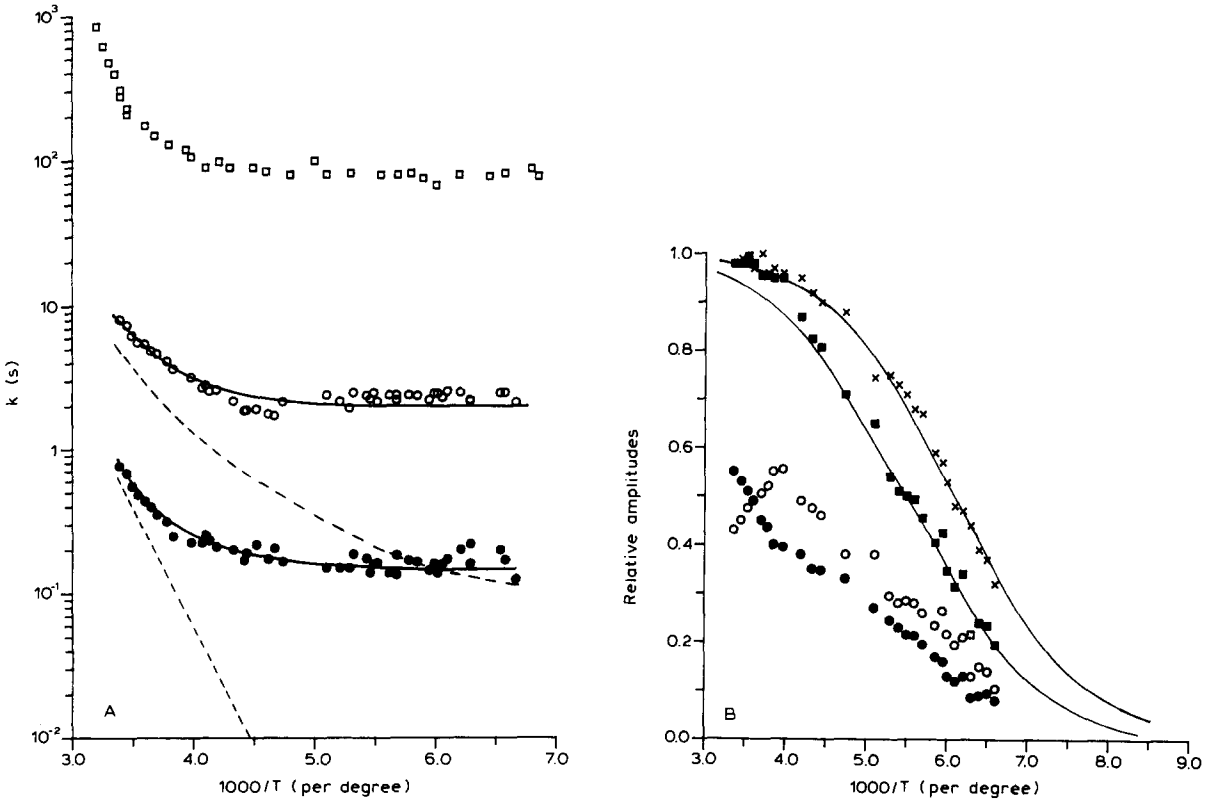

Fig. 4. The extended temperature dependence of the rates and amplitudes of recovery of photoinduced $C^+_{H1}Q^-_A$ and $C^+_{H2}Q^-_A$. 30 μM reaction centers, 0.1% Triton X-100, 100 mM NaCl, 10 mM CHES, 10 μM ascorbate, 4 mM *o*-phenanthroline (pH 9.0), diluted to 60% ethylene glycol. (A) The recovery rates: (○) fast phase: the rate of recovery of C^+_{H1}; (●) slow phase: the rate of recovery of C^+_{H2}. The rate of recovery of $P^+Q^-_A$, taken from Ref. 12, is also shown (□). The curves were constructed as described in the text using Eqns. 1 and 2 (solid lines), and Eqns. 3 and 4 (broken lines). (B) The recovery amplitudes: (○) fast phase amplitude: recovery of C^+_{H1}; (●) slow phase amplitude, recovery of C^+_{H2}; (■) sum of the two recovery amplitudes; (×) initial signal amplitude ($C^+Q^-_A$). The solid lines show fits for the total recovery amplitude and the initial amplitude, assuming equilibrium between an active and inactive conformation of the cytochromes, with $\Delta H = -0.117$ eV and $\Delta S = -0.63$ (left curve) or -0.70 (right curve) meV per degree.

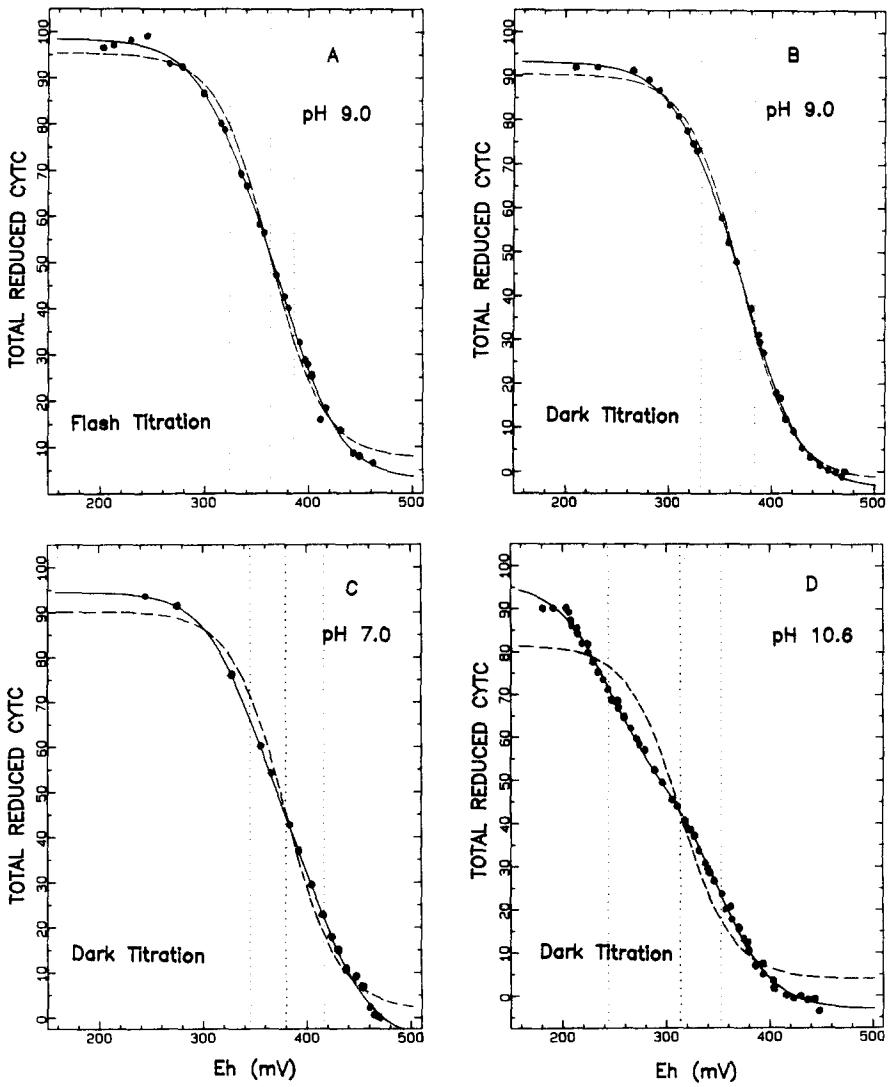

Fig. 5. Equilibrium redox titrations of the high potential cytochromes *c*. 2 μM reaction centers, 0.05% Triton X-100, 100 mM NaCl, 20 μM ubiquinone, and 10 mM Mops (pH 7.0), or 10 mM CHES (pH 9.0) or 10 mM CAPS (pH 10); $T = 296$ K. Mediators included 50 μM diaminodurene and 50 μM *N,N,N′,N′*-tetramethyl-*p*-phenylenediamine. The solution redox potential was varied by small additions of ferricyanide or ascorbate; data were obtained by oxidative and reductive titration. (A) Flash titration, pH 9.0; (B–D) dark titrations, pH 9.0, 7.0 and 10.7. Solid curves are fits with two one-electron components, with E_m values of 325 and 385 mV (A), 330 and 383 mV (B), 345 and 413 mV (C), and 245 and 352 mV (D). Dashed curves are fits to one one-electron component with E_m values of 363 mV (A), 366 mV (B), 378 mV (C) and 315 mV (D).

DW-2 spectrophotometer by monitoring absorbance at 558 nm, where both cytochrome *c*-559 and cytochrome *c*-556 absorb, versus an oxidized reference sample. Fig. 5B–D shows three titration curves at pH 7.0, 9.0 and 10.6. A second method involved measuring the total flash-induced optical absorption change at 558 nm, in the presence of ubiquinone and without *o*-phenanthroline. Under these conditions, after four saturating flashes, the total absorbance change at 558 nm provides a measurement of the reduced cytochrome *c* content before the flash at the given redox potential. Fig. 5A shows a flash titration curve at pH 9.0.

The results of dark titrations and flash titrations agreed well. The titration curves were nicely fit by two one-electron components (solid curves in Fig. 5), and not by one one-electron component (dashed curves in Fig. 5). The two components clearly correspond to the two high-potential hemes, cytochrome *c*-559 and cytochrome *c*-556, previously observed in kinetic measurements [6,7].

In order to establish the role of the two high-potential cytochromes in the flash-induced decay kinetics, observed at 558 nm, we titrated the fast and slow components by changing the redox potential. Fig. 6A and C show titrations of the amplitude of the slow component (at pH 9.0 and 10.7). The data were well fit by one one-electron component with a midpoint potential (E_m) in good agreement with the E_m of cytochrome *c*-556 obtained in dark and flash titrations. In contrast, the amplitude of the fast component increased with

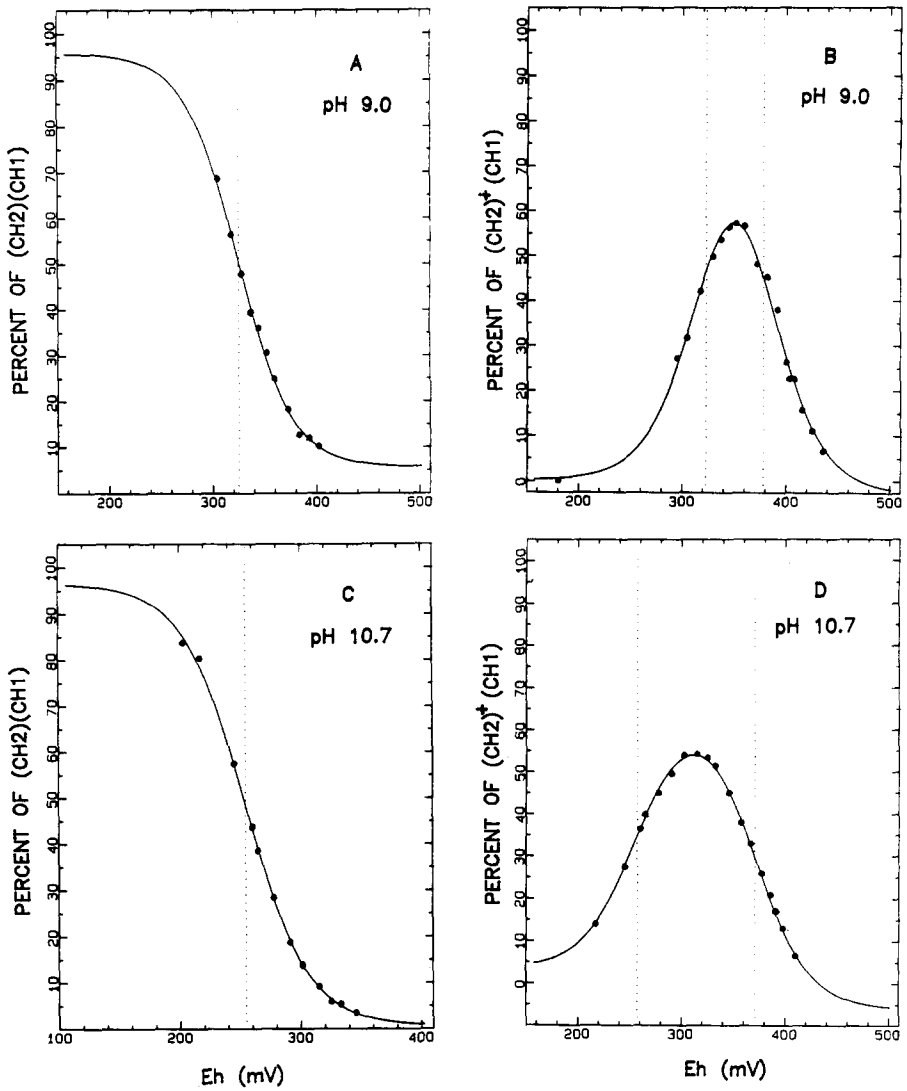

Fig. 6. Equilibrium redox titrations of the amplitudes of the phases of cytochrome c^+ recovery. 2 μM reaction centers, 0.05% Triton X-100, 100 mM NaCl, 4 mM *o*-phenanthroline and 10 mM CHES (pH 9.0) or 10 mM CAPS (pH 10.7); $T = 296$ K. The solution redox potential was varied by small additions of ferri- and ferrocyanide. (A, C) Titration of the slow phase, which is a measure of the state $C_{H2}C_{H1}$ before the flash, at pH 9.0 and 10.7, respectively. The solid curves are fits to one one-electron component with E_m values of 325 mV (A) and 252 mV (C). (B, D) Titration of the fast phase, which is a measure of the state $C^+_{H2}C_{H1}$ before the flash, at pH 9.0 and 10.7, respectively. The solid curves were fit with two one-electron components with E_m values of 323 and 379 mV (B), and 257 and 370 mV (D).

increasing E_h up to a maximum at 300–360 mV, depending on pH, and then decreased as the E_h was increased further. Fig. 6B and D show two such titration curves at pH 9.0 and 10.7, respectively. The data were fit by two one-electron components with E_m values in good agreement with those obtained for cytochrome *c*-559 and cytochrome *c*-556 in dark and flash titrations.

These results indicated that the two components in the decay kinetics arise from cytochrome *c*-559 (C_{H1}) and cytochrome *c*-556 (C_{H2}). In Fig. 6A and C the state under titration is $C_{H2}C_{H1}$: as the E_h is raised, C_{H2} is oxidized and the population of reaction centers in the state $C_{H2}C_{H1}$, before the flash, decreases. The kinetics after the flash, therefore, convert from the slow recombination of $C^+_{H2}C_{H1}Q^-_A$ to the fast kinetics of $C^+_{H2}C^+_{H1}Q^-_A$ recombination. In Fig. 6B and D the state $C^+_{H2}C_{H1}$ is titrated: at low E_h, most of the reaction centers are in the state $C_{H2}C_{H1}$ and the population of $C^+_{H2}C_{H1}$ is small. The flash-induced kinetics therefore reveal the slow recombination of $C^+_{H2}C_{H2}Q^-_A$. As the E_h is raised, more C_{H2} is oxidized and the population of $C^+_{H2}C_{H1}$ before the flash increases; as a result, the amplitude of the fast component increases. When E_h is raised further, both of the high potential hemes become oxidized, generating $C^+_{H2}C^+_{H1}$ before the flash. The dominant flash-induced state then becomes $P^+Q^-_A$, which recombines too fast to be detected in the same time range as the cytochrome recovery, and the amplitude of fast $C^+_{H2}C^+_{H1}Q^-_A$ recombination decreases. At pH values

lower than 8, this kind of titration behavior could not be observed because ferrocyanide, added during the titration to change E_h, can donate electrons to P^+ at low pH [14], interfering with the kinetics. The small amounts of ferricyanide, present initially, can also interfere due to the rapid reoxidation of Q_A^- that this agent can effect below pH 9 [14].

pH dependence of E_m of the cytochromes c and the primary donor

The pH dependence of the equilibrium midpoint potentials (E_m) of P and the high-potential cytochromes *c* are shown in Fig. 7. The cytochrome E_m data obtained by the three different methods were in good agreement. For C_{H1} and C_{H2}, at pH 7.0 and 296 K, the E_m values are 400 mV and 335 mV, respectively. These values are reasonably consistent with those reported by Dracheva et al., 390 mV and 320 mV [7]. The E_m values of the two high-potential cytochromes *c* were pH independent at pH values below 8.5. Above pH 8.5, the E_m of C_{H1} was slightly pH dependent (Fig. 7, middle curve), and the E_m of C_{H2} was distinctly pH dependent with a slope approaching −60 mV/pH unit above an apparent p*K* on the reduced form at about pH 9.5 (Fig. 7, lower curve).

The redox properties of the primary donor were obtained by titration of the flash-induced P^+ signal, observed at 450 nm. The E_m of P^+/P was 505 mV at pH 9.0 and was pH dependent above pH 7, with an average slope of about −30 mV/pH unit (Fig. 7, upper curve). This is a stronger pH dependence than observed for the $E_m(P^+/P)$ in chromatophores of *Rps. viridis* and of several other species [15,16].

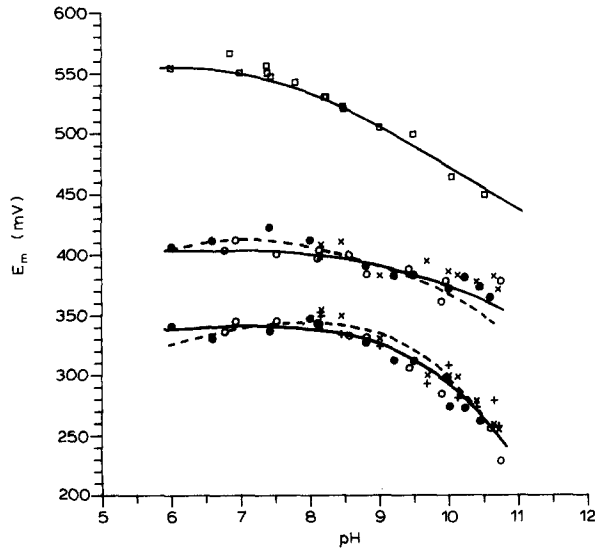

Fig. 7. The dependence on pH of the redox midpoint potentials of P (top), C_{H1} (middle) and C_{H2} (bottom). E_m of P^+/P (□) was assayed via the flash induced absorbance change at 450 nm; E_m values of C^+_{H1}/C_{H1} and C^+_{H2}/C_{H2} were determined by three different techniques; (●) flash titration as in Fig. 5A, (○) dark titration as in Fig. 5B, C and D, (+) kinetic analysis as in Fig. 6A and C (C_{H2}), (×) kinetic analysis as in Fig. 6B and D (C_{H1} and C_{H2}). Solid curves were used to calculate the solid curves in Fig. 2. Dashed curves were calculated as described in the text.

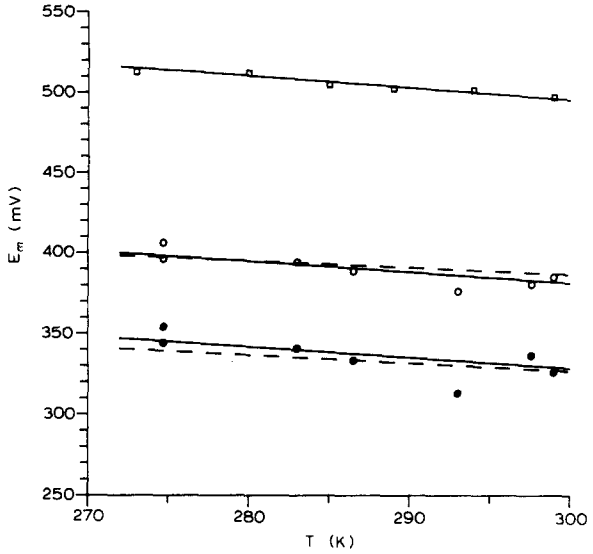

Fig. 8. The dependence on temperature of the redox midpoint potentials of P, C_{H1} and C_{H2}. (□) E_m of P^+/P; E_m values of C^+_{H1}/C_{H1} (○) and C^+_{H2}/C_{H2} (●) measured by flash titration as in Fig. 5A. Solid lines are least-square fits and were used to calculate the solid curves in Figs. 3 and 4A. Dashed lines were calculated as described in the text.

Temperature dependence of E_m of the cytochromes c and the primary donor

The temperature dependence of the midpoint potentials of P, C_{H1} and C_{H2} was measured by the flash titration method, at pH 9 (Fig. 8). The data shown are corrected for the temperature dependence of the reference electrode (see Materials and Methods). The buffer used (CHES) has a very low temperature coefficient (−0.009 pH per degree; Ref. 17) and the corrections arising from this were further minimized because the midpoint potentials are not strongly pH-dependent in this region (Fig. 7). The E_m of C^+_{H1}/C_{H1} decreased linearly with decreasing temperature, yielding a standard entropy of reduction (ΔS^0) of −0.66 meV per degree, determined from the slope, and a standard enthalpy (ΔH^0) of −579 meV, given by the intercept (E_m as $T \rightarrow 0$ K) (Fig. 8, open circles). The E_m of C^+_{H2}/C_{H2} decreased linearly with decreasing temperature, yielding, in the same fashion, $\Delta S^0 = -0.62$ meV per degree and $\Delta H^0 = -513$ meV (Fig. 8, filled circles). The temperature dependence of the E_m of P^+/P was also linear, with $\Delta S^0 = 0.72$ meV per degree and $\Delta H^0 = -709$ meV.

Discussion

The pathways of charge recombination of cytochrome $c^+Q_A^-$

The decays of the photoinduced high potential cytochrome c^+ and Q_A^- had the same kinetic character-

istics (Fig. 2), supporting the intramolecular nature of the process as the charge recombination of cytochrome $c^+Q_A^-$. Over a range of redox potentials, the observed decay of cytochrome $c^+Q_A^-$ is biphasic, as in Fig. 1, showing that there are two kinds of charge recombination. The fast phase corresponds to the charge recombination of $C_{H2}^+C_{H1}^+Q_A^-$, and the slow phase to the charge recombination of $C_{H2}^+C_{H1}Q_A^-$.

The temperature dependence of each cytochrome $c^+Q_A^-$ recombination process exhibited two distinct domains: a region of temperature dependence in the ambient temperature range (Figs. 3 and 4A), and temperature independence at low temperature (Fig. 4A). A very similar overall temperature dependence was reported for recombination of the $P^+Q_A^-$ state, both in RC's from *Rps. viridis* [12] and in *Rhodobacter sphaeroides* RC's with non-native quinones as Q_A [12,18]. This behavior was accounted for by two independent recombination processes for $P^+Q_A^-$: a thermally activated route via the energetically elevated state P^+I^-, dominant at higher temperatures, and a direct activationless recombination seen at low temperatures [12]. We propose here that decay of the cytochrome $c^+Q_A^-$ states occurs via thermal repopulation of the $P^+Q_A^-$ state, which then recombines rapidly (k_P is about 10^3 s^{-1}) to the ground state. Decay of $C_{H2}^+C_{H1}Q_A^-$ also requires thermal equilibrium between the states $C_{H2}^+C_{H1}$ and $C_{H2}C_{H1}^+$. These indirect pathways are in competition with very slow, direct electron tunneling recombinations of $C_{H2}^+Q_A^-$ with a rate k_{H2}^0, and of $C_{H1}^+Q_A^-$ with a rate k_{H1}^0.

The overall scheme for this is:

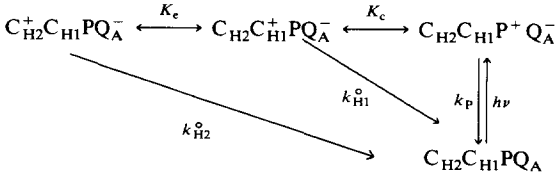

where K_e is the equilibrium constant for electron transfer between the two high-potential cytochromes c, k_P is the recovery rate of $P^+Q_A^-$ when the cytochromes are reduced and K_c is the equilibrium constant for the electron to lie on either P or C_{H1}. From the scheme above, assuming the electron transfer equilibria are established rapidly compared to the back reaction of $P^+Q_A^-$, the observed rate of decay of the state $C_{H2}^+Q_A^-$ is given by:

$$k_{H2}^{app} = \frac{k_P + K_c(k_{H1}^0 + K_e k_{H2}^0)}{1 + K_c(1 + K_e)} \quad (1)$$

If C_{H2} is oxidized before the flash, the reaction center is in the state $C_{H2}^+C_{H1}^+PQ_A^-$ after the flash. In this case, the observed recombination is described by the following scheme:

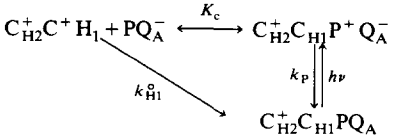

The rate of decay of the state $C_{H2}^+C_{H1}^+PQ_A^-$ is given by:

$$k_{H1}^{app} = \frac{k_P + K_c k_{H1}^0}{1 + K_c} \quad (2)$$

From Eqns. 1 and 2, the observed charge recombination rates, k_{H2}^{app} from $C_{H2}^+Q_A^-$ (k_{slow}) and k_{H1}^{app} from $C_{H1}^+Q_A^-$ (k_{fast}), can be calculated if the five variables in the equations are known.

From the available data for K_c, K_e, k_P, k_{H1}^0 and k_{H2}^0, the pH and temperature dependences of the fast and slow phases of cytochrome c^+ recovery were calculated. Beginning with the simple view of no redox-linked electrostatic interactions, the equilibrium constants, K_c and K_e, can be calculated from the difference in E_m values for P and C_{H1}, and for C_{H1} and C_{H2}, respectively, using the relation: $RT \ln K = nF\Delta E_m$. The pH and temperature dependences of K_c and K_e in isolated reaction centers were calculated from the data of Figs. 7 and 8, using values described by the solid lines, fitted to the data. The low-temperature dependences were obtained by linear extrapolation of the data of Fig. 8.

The rate of charge recombination in the state $C_{H2}C_{H1}P^+Q_A^-$, when the cytochromes c are reduced (k_P), is not experimentally accessible as the reduced cytochromes donate much faster than the recombination reaction. As a reasonable measure of k_p, we take the rate of recovery of P^+, in isolated reaction centers with a single quinone, when all the bound cytochromes c are chemically oxidized before the flash (k_P):

The choice of k_P is complicated by the fact that the actual kinetics of $P^+Q_A^-$ recombination are biphasic over much of the pH range [19]. This was suggested to reflect the rapidity of the recombination (approx. 1 ms) which does not allow equilibration of various protonation states of the RC, after the flash. If this is correct, then it is appropriate to use an average value for k_P when considering the much slower cytochrome $c^+Q_A^-$ recombination. The average should be one that is weighted over the post-flash, equilibrium distribution of protonation states, but this is not accurately known. We have, therefore, taken values obtained by analysing the $P^+Q_A^-$ recombination kinetics as a single component [12].

The other two variables in the equations, $k_{H2}^0 = 0.15$ s^{-1} and $k_{H1}^0 = 1.85$ s^{-1}, were taken from the measured

rates at low temperature (Fig. 4A). We have assumed them to be temperature independent. This assumption is not precise because, in general, activationless processes, and even tunneling rates, are also temperature dependent. However, the expected temperature dependence is small [20].

With these data, we have calculated the apparent rates of recombination for $C^+_{H2}C_{H1}PQ^-_A$ from Eqn. 1, and for $C^+_{H2}C^+_{H1}PQ^-_A$ from Eqn. 2, as either a function of pH (Fig. 2, solid curves) or temperature (Figs. 3 and 4A, solid curves). In both cases the calculated curves correlate well with the measured recombination rates.

The requirement for the existence of direct routes of recovery is clearly seen at low temperature. If we assume that the thermally activated route is the only pathway, we obtain for the expected rate of $C^+_{H2}C_{H1}PQ^-_A$ recovery:

$$k^{app}_{H2} = \frac{k_P}{1 + K_c(1 + K_e)} \tag{3}$$

and for the rate of $C^+_{H2}C^+_{H1}PQ^-_A$ recovery:

$$k^{app}_{H1} = \frac{k_P}{1 + K_c} \tag{4}$$

where the symbols are as for Eqns. 1 and 2. Using Eqns. 3 and 4 to fit the measured data yields a large mismatch at low temperature (broken lines, Fig. 4A). A fit to the low temperature data is only possible by taking account of the direct recombination routes for $P^+Q^-_A$ [12], $C^+_{H2}Q^-_A$ and $C^+_{H1}Q^-_A$, as in Eqns. 1 and 2 (solid line, Fig. 4A).

pH dependence of charge recombination of cytochrome $c^+Q^-_A$

From the model given above and Eqns. 1 and 2, it can be seen that the pH dependence of the charge recombination rates of cytochrome $c^+Q^-_A$ shown in Fig. 2 is due to the pH dependence of k_P and of the midpoint potentials of C_{H1}, C_{H2} and P. The good agreement with this prediction, shown in Fig. 2, would appear to vindicate the choice of a single component value for k_P, as discussed above. It should be noted that the calculated rates are very sensitive to the values of the midpoint potentials, and a difference in ΔE_m of 5 mV would yield markedly different results. The goodness of fit of the model is well supported by back-calculating the E_m/pH behavior of C_{H1} and C_{H2} using data points from the rates vs. pH (Fig. 2) and for $E_m(P^+/P)$ vs. pH (Fig. 7, top). This is shown by the dashed lines in Fig. 7, and clearly falls within the scatter of the measured E_m values. Similar treatment of the temperature dependence data (taking the rates from Fig. 3 and $E_m(P^+/P)$ from Fig. 8 (top)) yields the dashed lines in Fig. 8.

The pH dependences of the E_m's of P^+/P and the cytochromes are noteworthy, in their own right. The E_m of P^+/P is considerably more pH dependent than has been reported for this couple in chromatophores, either of *Rps. viridis* or of other species and, indeed, this couple has often been considered to be approximately pH-independent [15]. However, recent work on RCs from *Rb. sphaeroides* has clearly shown the primary donor to have significant redox-linked H^+ binding properties which do lead to a significant pH dependence of the E_m for this couple [21]. It was also found that the protonation behavior and, hence, the pH dependence of the equilibrium redox properties of the primary donor and the quinones was substantially different from that reported for chromatophores [22], implying a significant sensitivity of the redox-linked protonation events to the environment [21].

The E_m's of the cytochromes also showed some pH dependence, and for C_{H2} (cytochrome *c*-556) it approached -60 mV/pH at high pH. Such behavior is quite common for *c*-type cytochromes, although most reports have been for soluble species [23–26]. For cytochromes *c* and c_2 the onset of pH dependence is associated with a major structural change in which one of the axial ligands (Met) of the heme group is displaced, resulting in a structure that is incompetent in electron transfer [24]. Fig. 9 shows that similar failure occurs in the photooxidation of the reaction center cytochromes

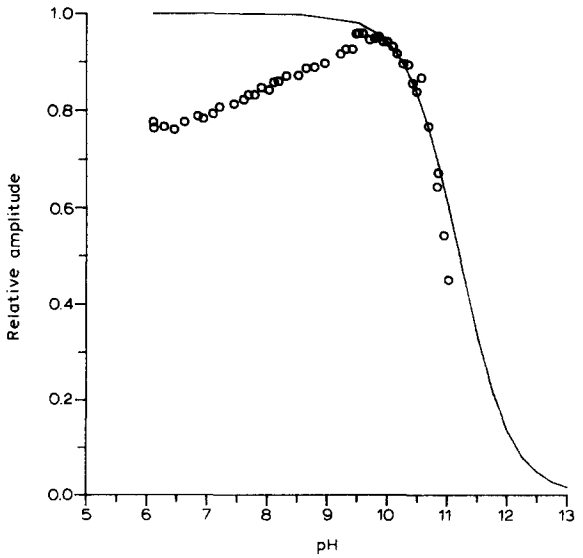

Fig. 9. The dependence on pH of the initial amplitude of cytochrome oxidation following a single flash. Conditions as for Fig. 2. The solid line is drawn according to the Henderson-Hasselbalch equation for a single group titrating with $pK = 11.2$.

of *Rps. viridis* at high pH. The fall-off in amplitude at pH values above 10 roughly follows a simple titration curve with apparent pK of 11.2. (The slight decrease in turnover as the pH is lowered below 10 is due to the progressive increase in E_h of the medium that accompanies acidification, resulting in partial oxidation of C_{H1}.) In the case of mitochondrial cytochrome *c*, the conformational and ligand changes that occur at high pH are accompanied by a substantial decrease in redox midpoint potential as well as changes in kinetic competence [24]. A similar change in E_m for C_{H1} in the reaction center, coupled to an apparent pK of 11.2 (Fig. 9), would be insignificant in the pH range of Fig. 7.

Temperature dependence of charge recombination of cytochrome $c^+Q_A^-$

A striking feature of the two phases of recombination is the very similar temperature dependences of the rates, which maintain a ratio close to 10 at all temperatures. The reaction schemes described above permit calculation of the activation energies for each phase, in the ambient temperature range. The apparent activation energy for $P^+Q_A^-$ recombination (the slope of the data in Fig. 3) is 0.125 eV and the electron transfers involved in populating this species from the oxidized cytochromes should add the enthalpy of the equilibria, K_c and K_e, to give the activation energies for the fast and slow cytochrome $c^+Q_A^-$ recombination processes. These are obtained after subtraction of the contributions from the activationless paths. For $C_{H1}^+Q_A^-$ this simply means subtracting k_{H1}^0, but for $C_{H2}^+Q_A^-$ there is, in addition to k_{H2}^0, a significant contribution from the direct recombination of $C_{H1}^+Q_A^-$, populated in a temperature dependent manner by equilibration with $C_{H2}^+Q_A^-$ but recombining via a temperature independent route. After correction for these routes (shown as dashed lines in Fig. 3), the resulting activation energies are 0.23 eV for $C_{H1}^+Q_A^-$, and 0.32 eV for $C_{H2}^+Q_A^-$. These may be compared with values of 0.25 eV and 0.32 eV, respectively, obtained by adding the appropriate differences in redox enthalpies (ΔH^0, from the temperature dependence of the midpoint potentials (Fig. 8)) to the apparent activation energy for $P^+Q_A^-$. This constitutes reasonable agreement, considering the substantial errors involved in the large extrapolations (to 0 K) necessary for obtaining ΔH^0 values from the Fig. 8.

At low temperatures, both phases appear to be activationless and the 10-fold difference in rates is remarkable if the low-temperature processes are considered to reflect direct recombination events. The distances involved in the recombination of $C_{H1}^+Q_A^-$ and $C_{H2}^+Q_A^-$ are large (approx. 50 and 80 Å center-to-center, respectively) and the additional 30 Å for the recombination of $C_{H2}^+Q_A^-$, compared to $C_{H1}^+Q_A^-$, would cause a massive decrease in the rate if the same, significant barrier height were maintained for both processes. For a barrier height of 1 eV (roughly appropriate for the intervening, potentially redox-active material, such as bacteriochlorophyll or bacteriopheophytin, etc.), the distance dependence of the electronic overlap can be given by an exponent factor of about 1 $Å^{-1}$ [20], leading to an expected decrease in rate of thirteen orders of magnitude over 30 Å. The much weaker distance dependence, observed here for the two high-potential heme recombination reactions, may point to the involvement of the intervening low-potential heme even at low temperature. Although thermal access to the low-potential heme must become impossible at low temperatures, the heme still presents a significant electron affinity compared to the non-redox material of the protein. Thus, the barrier height for tunnelling in this section of the path may be taken, roughly, as the difference in redox potentials between C_{H2} and C_{L1} ($\Delta E_m < 0.3$ V), instead of, say, 3–6 eV, for the non-redox material, or 1 eV used above for the material between C_{H1} and Q_A. This would strongly counteract the rate decrease expected from the increased distance.

The suggested role of the low-potential heme in lowering the barrier and extending the wave function of the distal high-potential heme, is similar to that proposed for the role of the monomer bacteriochlorophyll in the primary events (popularly referred to as superexchange) [27] and should not be considered exotic. A possible involvement of the low-potential heme is also suggested by data for the forward electron transfer from C_{H2} to C_{H1} at low temperature (Neshich, G., DeVault, D. and Wraight, C.A., unpublished results).

The amplitudes of the kinetic components associated with $C_{H2}^+C_{H1}^+$ (A_{fast}) and $C_{H2}^+C_{H1}$ (A_{slow}) changed with temperature (Fig. 4B). As the temperature was decreased from 300 K, A_{fast} first increased, but at temperatures below about 250 K it decreased. A_{slow}, on the other hand, decreased continuously with decreasing temperatures. The behavior at temperatures above 250 K is consistent with an effect via the ambient E_h increasing with decreasing temperature due to temperature dependence of the mediator and poising redox couples. So long as the sample remains liquid, permitting ongoing equilibration, an increase in E_h during cooling could cause an increase in $C_{H2}^+C_{H1}$ in the dark. Consequently, A_{fast} would increase and A_{slow} decrease. At temperatures below 250 K, the sample is frozen and the reaction centers cannot equilibrate further with the solution. As a result, any changes in the ambient E_h cannot affect the redox state of the reaction center.

In these terms the changes in A_{fast} and A_{slow}, in the 300–250 K range, are of trivial origin. A potentially more significant result is the steady decrease in the net amplitude of cytochrome oxidation, below 250 K, during which the relative amplitudes, A_{fast} and A_{slow}, remain essentially constant. A similar fall-off in recovery amplitude was seen at 554 and at 558 nm (not shown),

consistent with the relative insensitivity of the difference spectrum for the high-potential cytochromes to temperature (Ref. 30; Neshich, G., DeVault, D. and Wraight, C.A., unpublished results). The signal following a single flash was almost gone at temperatures below 140 K but could be slightly increased by giving several closely spaced (< 100 ms) flashes in a row. The extent of the enhancement was variable from sample to sample, however, and was mostly due to lack of light saturation by a single flash rather than a decrease in photochemical yield. When the sample was warmed up, the net amplitude of cytochrome oxidation and A_{fast} and A_{slow} recovered reversibly.

Concurrent measurements of the resolved forward kinetics of cytochrome *c* oxidation (Neshich, G., Devault, D. and Wraight, C.A., unpublished results) show that the initial transient, following a laser flash ($P^+Q_A^-$), increases at low temperature due to an enhanced electrochromic response of the bacteriopheophytin spectrum to Q_A^- [8]. This contribution is in the opposite direction to that of cytochrome c^+, so the net absorbance attributable to cytochrome c^+ Q_A^- is smaller. The effect is not sufficient to account for the almost total loss of flash induced signal observed here.

The loss of amplitude cannot simply result from the competition between $P^+Q_A^-$ recombination and electron transfer from C_{H1} to P^+. At 150 K, the rate of charge recombination of $P^+Q_A^-$ is about 120 s^{-1}, whereas the rate of electron transfer from C_{H1} to P^+ is about $5 \cdot 10^3$ s^{-1} (Neshich, G., DeVault, D. and Wraight, C.A., unpublished results). This conclusion contrasts with an earlier proposal from this lab, based on a rate of $2.8 \cdot 10^2$ s^{-1} for electron transfer from C_{H1} at 125 K [6]. It now appears that this slower value corresponds to the interheme electron transfer between C_{H2} and C_{H1} (Neshich, G., DeVault, D. and Wraight, C.A., unpublished results). The decrease in net amplitude as the temperature decreases could arise from an equilibrium between two states of the RC-cytochrome complex, one active and one inactive with respect to electron transfer to P^+. This simple description puts constraints on the rate of interconversion between active and inactive conformations. (1) At low temperatures (less than 250 K), the interconversion must be slow compared to the $P^+Q_A^-$ recombination process (approx. 10 ms) and to the flash period in multiple flash measurements (approx. 0.1 s). (2) The interconversion rate must be fast compared to the equilibration time between measurements (approx. 5 min) in order for the temperature dependence to be reversible. This would also account for the observation that continuous illumination at liquid helium temperatures results in full oxidation of one equivalent of high-potential heme (cytochrome *c*-556) [30]. If such a model is applied, the equilibrium constant between the two states can be obtained from the net amplitude of flash induced cytochrome oxidation as a function of temperature:

$$\text{active} \longleftrightarrow \text{inactive}$$

$$K = \frac{1}{\text{amplitude}} - 1$$

where the signal amplitude is normalized to 1 at high (ambient) temperatures. The derived parameters are $\Delta H = -0.12$ eV, $\Delta S = -0.65$ meV per degree, and the expected dependence is given by the solid lines in Fig. 4B. The small difference in fitting parameters for the recovery amplitude and the initial amplitude (see legend to Fig. 4B) may indicate a distribution of conformational substates [31]. The calculated entropy change is quite large, as befits a conformational event. An interesting possibility is a structural change at the heme of C_{H1} such as that suggested to occur at high pH (see Fig. 9).

Since the relative proportions of fast and slow phases stayed constant while the total amplitude decreased, the effect seems to be restricted to the $C_{H1} \rightarrow P^+$ step and no such freezing out of the interheme electron transfer between C_{H2} and C_{H1} occurred. Furthermore, since k_{slow} and k_{fast} decreased in parallel, it would seem that K_e for the active conformation of C_{H1} is almost temperature independent, varying by less than 50% over the whole range of Fig. 4A. This is consistent with the observed dependence of the E_m's in the ambient temperature range (Fig. 8).

Charge interactions between redox centers

So far the possibility of electrostatic interactions between charged species has been explicitly ignored in order to use, directly, the measured redox midpoint potentials for estimating the electron-transfer equilibria of Schemes I and II. The agreement with the data is generally good. However, the compact nature of the reaction center renders this assumption suspect. Recent studies by Dracheva et al. [7] have given some direct evidence of the dielectric environment between the redox centers. Thus, in membranous preparations, the light-driven electron transfer through the reaction center generates approx. 37%, 37%, 16% and 5% of the total transmembrane potential difference at each of the charge separation steps: Q_A–I, I–P, P–C_{H1} and C_{H1}–C_{H2}. (The remaining 5% is associated with H^+ uptake to the quinone complex, but is only seen on even turnovers as quinol is produced.) The corresponding distances involved are roughly 15 Å, 15 Å, 21 Å and 29 Å, center-to-center [5,7]. If the geometry of the membrane system is approximated to that of a parallel plate capacitor, an effective dielectric constant can be derived for each segment. Furthermore, recent studies have shown substantial effects of large applied electric fields on the yield of $P^+Q_A^-$ formation [32]. This has been interpreted as arising predominantly from an effect on the P^+I^-

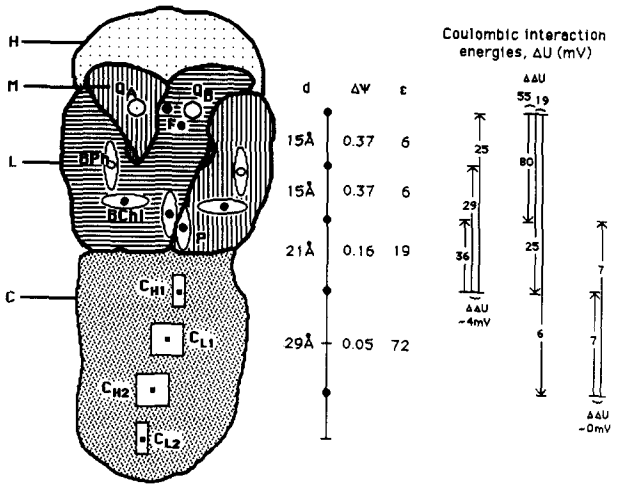

Fig. 10. *Schematic of electron-transfer steps within the Rps. viridis* reaction center. Distances between cofactors (Q_A, I (BPh), P, C_{H1} and C_{H2}) are for projections along the central axis of the RC and were taken from Refs. 5 and 7; membrane potential contributions ($\Delta\psi$) were taken from Ref. 7; effective dielectric constants (ε) were estimated as described in the text. The electrostatic interactions energies between charge pairs, ΔU, were calculated from Coulomb's law, and the differences are shown as $\Delta\Delta U$.

formation step, allowing estimation of an effective dielectric constant of 6 in this region (Alegria, G. and Dutton, P.L., personal communication). We have used this value to obtain an absolute value for the average dielectric constant in each segment of the electron-transfer pathway, as shown in Fig. 10. Also shown are the magnitudes of the electrostatic interactions (ΔU) between selected charge pairs, using the distances and dielectric constants shown.

Although the concept of dielectric constants in intramolecular interactions is contentious at a rigorous level of application [33,34], it would seem to be a useful starting point for assessing the possibility of perturbations of the equilibrium electron-transfer constants by nonequilibrium species. Thus, with the dielectric constants shown in Fig. 10, the presence of Q_A^- would significantly perturb ($\Delta\Delta U = 55$ mV) the electron transfer equilibrium (K_c) between P^+/P and C_{H1}^+/C_{H1}, as the estimated influence on P^+/P ($\Delta U = 80$ mV) is substantially larger than that on C_{H1}^+/C_{H1} ($\Delta U = 25$ mV). The effect of Q_A^- on K_e, arising from the differential influence on C_{H1}^+/C_{H1} and C_{H2}^+/C_{H2}, is also significant but not large ($\Delta\Delta U = 19$ mV). On the other hand, the very large dielectric constant that prevails in the region between C_{H1} and C_{H2} ($= 72$), essentially obliterates any possible influence of C_{H2}^+ on K_c.

The influence of C_{H1}^+/C_{H1} on k_P can also be estimated in this fashion. Any effect at room temperature is likely to be exerted via the magnitude of the redox free energy span (ΔG) between $P^+IQ_A^-$ and $P^+I^-Q_A$, according to [12]:

$$k_P = k_d \cdot e^{-\Delta G/RT} + k_T \quad (5)$$

This expression describes the $P^+Q_A^-$ recombination process as a single exponential derived from two competing pathways, an activated recombination via P^+I^- ($k_d = 2 \cdot 10^{-7}\,s^{-1}$, $\Delta G = 0.28$ eV) and an activationless process seen at low temperature ($k_T = 170\ s^{-1}$). From Fig. 10, it can be seen that the magnitude of the perturbation of ΔG by C_{H1}^+/C_{H1} is only 4 mV, which would result in only a 10% change in k_P.

The progressively larger apparent dielectric constants that prevail in the regions of the RC that extend out of the membrane, i.e., the $P-C_{H1}$ and $C_{H1}-C_{H2}$ spans of the electron-transfer pathway, suggest a significant effect of the solvent in determining this effective parameter. Since the current studies have been performed on isolated reaction centers, in aqueous detergent suspensions, it is reasonable to consider that the effective dielectric constants in the hydrophobic segments of the electron path could be significantly higher than those estimated for membrane preparations and that, consequently, the magnitudes of the electrostatic interactions would be much smaller. The good agreement between the observed behavior and that calculated from Eqns. 1 and 2, using measured equilibrium midpoint potentials and the measured value for k_P, supports this final analysis. However, the potential for significant perturbations between redox centers in membranous systems should be noted and will be examined future work.

We conclude that the correlation between the observed and calculated rates, as functions of both temperature and pH, supports a model in which $C_{H2}^+C_{H1}Q_A^-$ recovers by an indirect pathway, via $C_{H2}C_{H1}^+Q_A^-$ and $P^+Q_A^-$, and a direct pathway; $C_{H1}^+Q_A^-$ also recovers by both an indirect pathway, via the $P^+Q_A^-$ state, and by a direct pathway. The large distances involved in the direct recombination routes, observed at low temperature, present a challenge to current theories of electron transfer.

Acknowledgements

This work was supported by a grant from the National Science Foundation (DMB 86-17144). We would like to acknowledge helpful discussion with Darrell Fleischman concerning his unpublished work on these reactions.

References

1 Parson, W.W. and Ke, B. (1982) in Photosynthesis Energy Conversion by Plants and Bacteria (Govindjee, ed.), Vol. 1, pp. 331–386, Academic Press, New York.

2 Clayton, R.K. and Clayton, B.J. (1978) Biochim. Biophys. acta 501, 478–487.
3 Prince, R.C., Leigh, J.S., Jr. and Dutton, P.L. (1976) Biochim. Biophys. Acta 440, 622–636.
4 Deisenhofer, J., Epp, O., Miki, K., Huber, R. and Michel, H. (1984) J. Mol. Biol. 180, 358–398.
5 Deisenhofer, J., Epp, O., Miki, K., Huber, R. and Michel, H. (1985) Nature 318, 618–624.
6 Shopes, R.J., Levine, L.M.A., Holten, D. and Wraight, C.A. (1987) Photosyn. Res. 12, 165–180.
7 Dracheva, S.M., Drachev, L.A., Kostantinov, A.A., Semenov, A.Yu., Skulachev, V.P., Arutjunjan, A.M., Shuvalov, V.A. and Zaberezhnaya, S.M. (1988) Eur. J. Biochem. 171, 253–264.
8 Shopes, R.J. and Wraight, C.A. (1985) Biochim. Biophys. Acta 806, 348–356.
9 Fleischman, D. (1978) Biophys. J. 21, 9a.
10 Prince, R.C., Tiede, D.M., Thornber, J.P. and Dutton, P.L. (1977) Biochim. Biophys. Acta 462, 467–490.
11 Wraight, C.A. (1979) Biochim. Biophys. Acta 548, 364–371.
12 Shopes, R.J. and Wraight, C.A. (1987) Biochim. Biophys. Acta 893, 409–425.
13 Lingane, J.J. (1958) Electroanalytical Chemistry, pp. 360–361.
14 Shopes, R.J. and Wraight, C.A. (1986) Biochim. Biophys. Acta 848, 364–371.
15 Prince, R. and Dutton, P.L. (1978) in The Photosynthetic Bacteria (Clayton, R.K. and Sistrom, W.R., eds.), pp. 439–453, Plenum Press, New York.
16 Case, G.D. and Parson, W.W. (1971) Biochim. Biophys. Acta 253, 187–202.
17 Good, N.E., Winget, G.D., Winter, W., Connolly, T.N., Izawa, S. and Singh, R.M.M. (1966) Biochemistry 5, 467–477.
18 Gunner, M.R., Robertson, D.E. and Dutton, P.L. (1986) J. Phys. Chem. 90, 3183–3195.
19 Sebban, P. and Wraight, C.A. (1989) Biochim. Biophys. Acta 974, 54–65.
20 DeVault, D. (1981) Q. Rev. Biophys. 13, 387–564.
21 Maroti, P. and Wraight, C.A. (1988) Biochim. Biophys. Acta 934, 329–347.
22 Petty, K.M., Jackson, J.B. and Dutton, P.L. (1979) Biochim. Biophys. Acta 546, 17–42.
23 Brandt, K.G., Parks, P.C., Czerlinski, G.H. and Hess, G.P. (1966) J. Biol. Chem. 241, 4180–4185.
24 Davis, L.A., Schejter, A. and Hess, G.P. (1974) J. Biol. Chem. 249, 2624–2632.
25 Pettigrew, G.W., Bartsch, R.G., Meyer, T.E. and Kamen, M.D. (1978) Biochim. Biophys. Acta 503, 509–523.
26 Prince, R.C. and Bashford, C.L. (1979) Biochim. Biophys. Acta 547, 447–454.
27 Michel-Beyerle, M.E., Plato, M., Deisenhofer, J., Michel, H., Bixon, M. and Jortner, J. (1988) Biochim. Biophys. Acta 932, 52–70.
28 Warshel, A., Russell, S.T. and Churg, A.K. (1984) Proc. Natl. Acad. Sci. USA 81, 4785–4789.
29 Seibert, M. and DeVault, D. (1971) Biochim. Biophys. Acta 253, 396–411.
30 Verméglio, A., Richaud, P. and Breton, J. (1989) FEBS Lett. 243, 259–263.
31 Debrunner, P.G. and Frauenfelder, H. (1982) Ann. Rev. Phys. Chem. 33, 283–299.
32 Popovic, Z.D., Kovacs, G.J., Vincett, P.S., Alegria, G. and Dutton, P.L. (1986) Biochim. Biophys. Acta 851, 38–48.
33 Gilson, M., Rashin, A., Fine, R. and Honig, B. (1985) J. Mol. Biol. 183, 503–516.